

TAUE: Training-free Noise Transplant and Cultivation Diffusion Model

Daichi Nagai^{1*} Ryugo Morita^{1*} Shunsuke Kitada¹ Hitoshi Iyatomi¹

¹Department of Applied Informatics, Graduate School of Science and Engineering, Hosei University, Tokyo, Japan
{daichi.nagai.9s@stu., iyatomi@}hosei.ac.jp

Abstract

Despite the remarkable success of text-to-image diffusion models, their output of a single, flattened image remains a critical bottleneck for professional applications requiring layer-wise control. Existing solutions either rely on fine-tuning with large, inaccessible datasets or are training-free yet limited to generating isolated foreground elements, failing to produce a complete and coherent scene. To address this, we introduce the Training-free Noise Transplantation and Cultivation Diffusion Model (TAUE), a novel framework for zero-shot, layer-wise image generation. Our core technique, Noise Transplantation and Cultivation (NTC), extracts intermediate latent representations from both foreground and composite generation processes, transplanting them into the initial noise for subsequent layers. This ensures semantic and structural coherence across foreground, background, and composite layers, enabling consistent, multi-layered outputs without requiring fine-tuning or auxiliary datasets. Extensive experiments show that our training-free method achieves performance comparable to fine-tuned methods, enhancing layer-wise consistency while maintaining high image quality and fidelity. TAUE not only eliminates costly training and dataset requirements but also unlocks novel downstream applications, such as complex compositional editing, paving the way for more accessible and controllable generative workflows.

1 Introduction

Diffusion models have revolutionized creative workflows by enabling the synthesis of photorealistic and intricate images from text prompts (Ho, Jain, and Abbeel 2020; Song, Meng, and Ermon 2020; Rombach et al. 2022; Hu et al. 2024). Yet, this transformative power is constrained by a critical limitation: they typically generate only single-layered, flat images. These flat images severely restrict post-hoc manipulation, as individual elements are inextricably fused. In professional domains such as art, design, and animation, where refining complex compositions is crucial, this lack of layer-wise control presents a significant bottleneck, forcing practitioners to engage in laborious manual segmentation and inpainting.

In response, most existing work has leveraged fine-tuning for layer-wise image generation. These methods attempt to

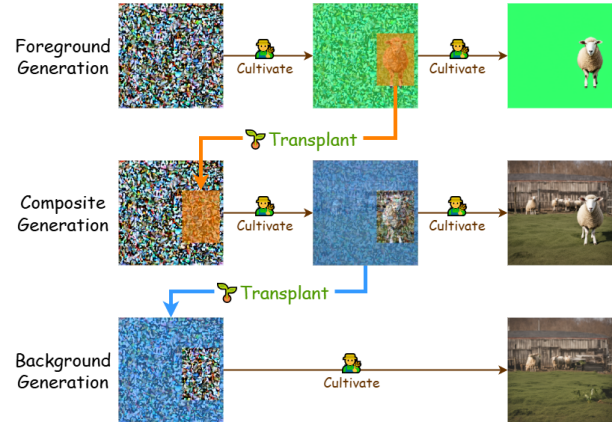


Figure 1: TAUE introduces a training-free method for layer-wise image generation. By transplanting an intermediate *seedling latent* from the foreground to the composite generation process, TAUE simultaneously produces a consistent foreground, background, and composite image.

denoise multiple layers simultaneously using masks (Zhang et al. 2023; Huang et al. 2024; Fontanella et al. 2024; Kang et al. 2025) or employ specialized alpha-channel autoencoders (Zhang and Agrawala 2024; Dalva et al. 2024; Huang et al. 2025a; Pu et al. 2025). While effective to some extent, these approaches depend on large-scale, curated datasets and prohibitive training costs. Critically, these datasets are often proprietary or inaccessible, creating a significant barrier to entry that hinders reproducible research and slows community progress. To circumvent this data dependency, training-free approaches have been explored (Quattrini et al. 2024; Morita et al. 2025; Zou et al. 2025). However, these methods focus exclusively on generating isolated foregrounds and do not attempt to produce a corresponding background. This inherently limits them to partial solutions, leaving a critical research gap for a framework capable of layer-wise image generation without requiring fine-tuning.

To address this gap, we propose the novel Training-free Noise Transplant and Cultivation Diffusion Model (TAUE). Inspired by Guo et al. (2024), TAUE introduces a novel mechanism that manipulates this initial noise to achieve semantically coherent, layer-wise image generation. Our core

*These authors contributed equally.

technique, Noise Transplantation and Cultivation (NTC), harvests intermediate latents from the diffusion processes and reuses them to cultivate coherent layers throughout the generation pipeline. First, foreground seedling noise is extracted from the foreground generation and transplanted into the initial noise for the composite generation. Then, background seedling noise is derived from the composite generation and used as the initial noise for background generation. This ensures semantic and structural coherence across layers, enabling consistent, multi-layered outputs—foreground, background, and composite—without requiring fine-tuning or additional datasets. By transplanting and cultivating latents at each stage, TAUE generates a coherent composite scene in which all layers align seamlessly. This approach eliminates the need for expensive fine-tuning and large datasets, while opening up new applications, such as complex compositional editing.

Extensive experiments demonstrate that TAUE achieves state-of-the-art results among training-free methods, improving layer-wise consistency while matching the quality of fine-tuned models. Our contributions are threefold: **(1)** We introduce TAUE, a novel framework for layered image generation that eliminates the need for fine-tuning and external datasets. **(2)** We propose NTC, which manipulates ancestral noise of the diffusion process. TAUE achieves natural coherence across layers that previous approaches could only approximate through large-scale training. **(3)** We demonstrate state-of-the-art performance in training-free layered image generation, enabling a range of previously intractable downstream applications.

2 Related Works

2.1 Initial Noise of Diffusion Model

Diffusion models turn Gaussian noise into structured data through a step-by-step refinement process. Tailoring the initial noise improves image fidelity and alignment, with recent studies focusing on optimal noise selection (Xu, Zhang, and Shi 2024; Wang et al. 2024; Guo et al. 2024; Eyring et al. 2024) and latent optimization (Chen et al. 2024a; Zhou et al. 2024; Qi et al. 2024). Furthermore, identifying optimal noise seeds and focusing on specific noise regions affect image quality and object placement (Ban et al. 2024; Han et al. 2025; Izadi et al. 2025), while noise manipulation enables advanced tasks for layout control (Shirakawa and Uchida 2024; Mao, Wang, and Aizawa 2023b), editing (Mao, Wang, and Aizawa 2023a; Chen et al. 2024b), and video generation (Wu et al. 2024; Morita et al. 2025).

Building on these insights, we propose a novel NTC method that embeds an object’s intermediate latent into the initial latent space. By aligning this noise’s distribution with the Gaussian prior, our method reconstructs the object while generating an entirely new background.

2.2 Layer-wise Image Generation

Layer-wise image generation is essential for professional applications that require fine-grained compositional control and editing. Fine-tuned approaches typically achieve this using special masks (Zhang et al. 2023; Huang et al. 2024;

	Fine-tuned		Training-free	
	LayerDiffuse	ART	Alfie	Ours
Background	✓	✓	✗	✓
Multi-object	✓	✓	✗	✓
Harmonization	✗	✗	✗	✓
Layout specification	✗	✓	✗	✓

Table 1: Qualitative capability comparison between our TAUE and well-established layer-wise image generation methods such as LayerDiffuse (Zhang and Agrawala 2024), ART (Pu et al. 2025), Alfie (Quattrini et al. 2024). TAUE uniquely enables training-free generation of complete scenes with background synthesis, multi-object disentanglement, semantic harmonization, and layout controllability surpassing both fine-tuned and training-free baselines.

Fontanella et al. 2024; Kang et al. 2025) or alpha-channel autoencoders (Zhang and Agrawala 2024; Dalva et al. 2024; Huang et al. 2025a; Pu et al. 2025). However, these methods rely heavily on large-scale, proprietary datasets, which limits their practicality and reproducibility.

Training-free alternatives (Morita et al. 2025; Quattrini et al. 2024; Zou et al. 2025) eliminate the need for data collection; however, they fail to produce complete scenes, generating only isolated foregrounds. In contrast, our approach is the first zero-shot, complete solution for layer-wise image generation without fine-tuning or data collection.

2.3 Layer Decomposition and Composition

An alternative to direct layered generation is post-hoc decomposition, where a flat image is broken into distinct layers. This research focuses on building large-scale datasets to train decomposition models. These datasets may offer either fine-grained part masks, which lack the transparency needed for flexible compositing (Liu et al. 2024), or full RGBA layers (Huang et al. 2025b). However, such datasets are often curated by other models and often fail to capture complex visual effects like soft shadows and reflections, limiting their utility for seamless editing (Burgert et al. 2024; Tudosi et al. 2024; Yang et al. 2025).

Moreover, beyond decomposition, harmonizing extracted layers into a cohesive image poses a distinct challenge. This step typically requires costly fine-tuning to blend lighting and color—a process that can alter the original appearance of elements (Winter et al. 2024; Zhang, Wen, and Shi 2020; Huang et al. 2025a). These dual challenges—dependence on large datasets and expensive harmonization—underscore fundamental limitations of this pipeline. In contrast, TAUE bypasses these issues by generating coherent foreground, background, and composite layers simultaneously in zero-shot fashion, ensuring consistency from the outset without datasets or post-hoc correction.

3 TAUE

TAUE utilizes Latent Diffusion Model (LDM) (Rombach et al. 2022) to achieve layer-wise image generation without requiring fine-tuning or additional datasets. In LDM such as

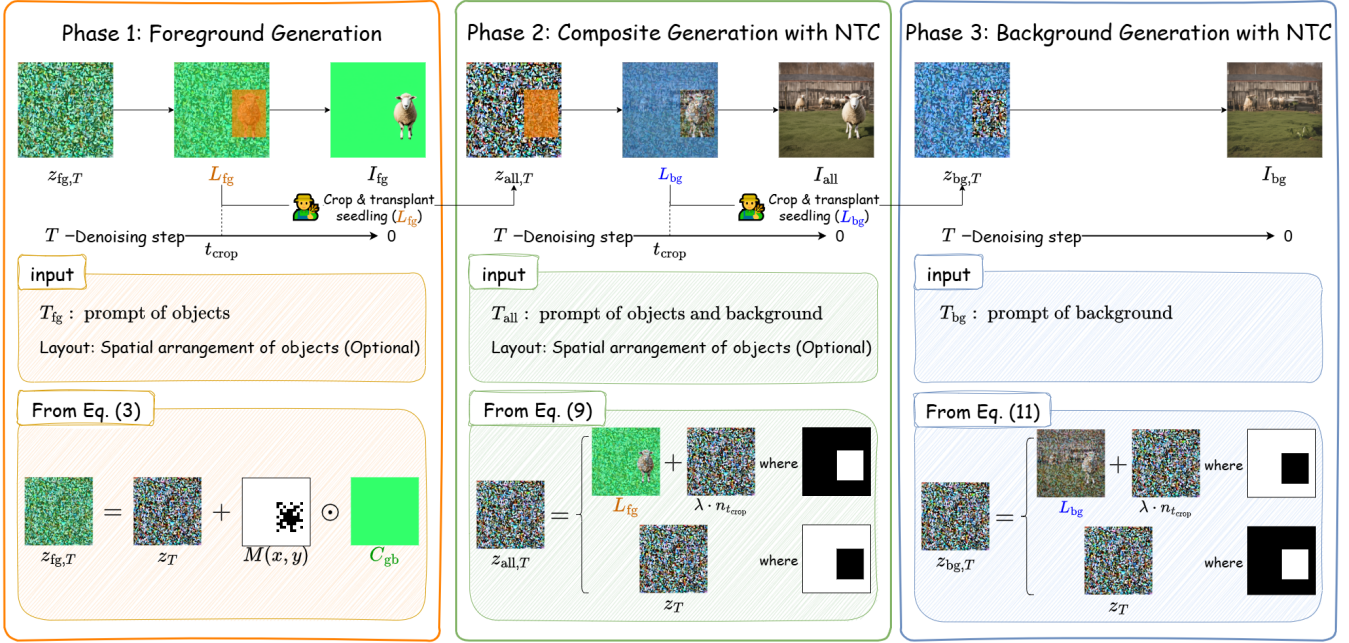


Figure 2: The generation process consists of three stages: (1) Foreground Generation, where an object is generated from noise and a seedling latent is extracted; (2) Composite Generation, where the seedling latent is transplanted into a new denoising trajectory to generate a full scene; and (3) Background Generation, where the background is reconstructed separately from the same noise. To ensure spatial and semantic consistency, we introduce an NTC strategy, which constrains the object region with fixed seedling noise during early denoising steps and gradually relaxes this constraint to produce a coherent composite.

Stable Diffusion (Rombach et al. 2022) and SDXL (Podell et al. 2023), the VAE encodes an RGB image into a latent representation $\mathbf{z} \in \mathbb{R}^{4 \times H/8 \times W/8}$, i.e. *four feature channels*. We follow the common 0-based indexing convention ($c = 0, 1, 2, 3$) when referring to individual channels.

As shown in Fig. 2 The process of TAUE is divided into three phases: (1) Foreground Generation, (2) Composite Generation with NTC, and (3) Background Generation with NTC. We use three distinct text prompts — T_{fg} , T_{bg} , and T_{all} — for foreground, background, and composite generation.

- (1) We generate the foreground object on a uniform background to obtain a clean foreground layer I_{fg} (§3.1). During this step, an intermediate foreground seedling latent L_{fg} is extracted, encoding structural and semantic features of the object.
- (2) L_{fg} is transplanted into the initial noise $z_{all,T}$ for composite generation, yielding both the background seedling latent L_{bg} and the composite scene I_{all} (§3.2).
- (3) L_{bg} is transplanted into the initial noise $z_{bg,T}$ for generating the background I_{bg} , ensuring consistency between the foreground, background, and composite scene (§3.3).

The final output comprises three distinct layers: the foreground I_{fg} , background I_{bg} , and composite scene I_{all} , forming a coherent image.

3.1 Foreground Generation

TAUE enables flexible multi-object generation, specifying object positions and sizes with a binary mask. However,

uniform binary masks often lead to rigid, box-shaped foregrounds due to their flat probability distribution.

To address this limitation, we introduce a probabilistic mask generation strategy that controls the likelihood of each pixel being included in the mask. Rather than uniformly sampling all pixels within a rectangular region, we define a spatial probability distribution that reflects the spatial importance of pixels within an object’s bounding box, i.e., the region intended for object generation.

Specifically, for a given bounding box centered at (o_x, o_y) with width w and height h , we define a radially symmetric Gaussian distribution confined to this region:

$$P(x, y) = \begin{cases} \exp\left(-\frac{1}{2\sigma^2} \left(\left(\frac{x-o_x}{w/2}\right)^2 + \left(\frac{y-o_y}{h/2}\right)^2 \right)\right) & \text{if } |x - o_x| \leq w/2, |y - o_y| \leq h/2 \\ 0 & \text{otherwise.} \end{cases} \quad (1)$$

Here, $P(x, y)$ serves as an *object retention score*, indicating how strongly the original noise at pixel (x, y) is preserved in this operation. High values of $P(x, y)$ help maintain the initial noise and thereby promote object synthesis in those areas. The parameter σ controls spatial falloff within the bounding box, and (o_x, o_y) specifies the center of the object’s intended region. Pixels outside the box are assigned zero probability, ensuring the mask is strictly confined to the object’s designated area.

This retention map is further scaled to a target range $[p_{min}, p_{max}]$ and compared with a randomly sampled value

$R(x, y)$ to generate a binary mask:

$$M(x, y) = \begin{cases} 1 & \text{if } R(x, y) > P(x, y) \\ 0 & \text{otherwise} \end{cases}. \quad (2)$$

As a result, pixels near the center of the bounding box are less likely to be masked, while those near the edges are more likely to be included in the mask.

Inspired by TKG-DM (Morita et al. 2025), we blend a green background latent vector $C_{\text{gb}} = [0, 1, 1, 0]$ into the initial noise $z_T \sim N(0, 1)$ within the generated mask M :

$$z_{\text{fg},T} = (1 - M) \odot z_T + M \odot ((1 - \alpha)z_T + \alpha C_{\text{gb}}), \quad (3)$$

where α is the mixing parameter controlling the contribution of the green background. Here $C_{\text{gb}} \in \mathbb{R}^4$ matches the latent channel count; we set $c = 1, 2$ (roughly corresponding to the G and B axes after decoding, in an RGB-like layout) to 1 and leave $c = 0, 3$ at 0. The resulting latent $z_{\text{fg},T}$ is then used in the vanilla denoising process with foreground text prompt T_{fg} to obtain I_{fg} .

We cache the latent tensor at the crop timestep t_{crop} , which corresponds to a predefined denoising progress ratio r_{crop} . Specifically, t_{crop} is defined as the timestep at which r_{crop} of the total denoising process has been completed, measured along the reverse time axis of the scheduler. We then define:

$$L_{\text{fg}} = z_{\text{fg},t_{\text{crop}}} \in \mathbb{R}^{4 \times H/8 \times W/8}, \quad (4)$$

where $t_{\text{crop}} = \lfloor T \cdot (1 - r_{\text{crop}}) \rfloor$. This cached latent, hereafter called the *seedling latent*, encodes foreground geometry and semantics and will be re-injected in the subsequent stages.

3.2 Composite Generation with Noise Transplantation and Cultivation (NTC)

Just as a seedling can shape the ecosystem it grows in, transplanting latent noise from foreground into new generative processes can guide the formation of coherent visual scenes. In this phase, we generate a coherent composite scene by transplanting the seedling latent L_{fg} from the foreground phase and cultivating it within the diffusion process. This is guided by an object mask and reinforced through spatially-aware attention and noise control mechanisms.

Object Region Mask We begin by localizing the object region in the latent space using two complementary signals: latent channel activations and cross-attention maps. During foreground generation, a green latent vector C_{gb} is injected into the background region of the initial latent, elevating activations in channels $c = 1$ and $c = 2$. The object region, unaffected by this injection, exhibits low activation in these channels. We construct a smooth activation map as:

$$v_{\text{gb}}(x, y) = \mathcal{G}_\sigma(L_{\text{fg}}^{(1)} + L_{\text{fg}}^{(2)}), \quad (5)$$

where \mathcal{G}_σ is Gaussian blur operator with parameter σ , and $L_{\text{fg}}^{(1)}$ and $L_{\text{fg}}^{(2)}$ denote the 1st and 2nd channels of the seedling latent L_{fg} after foreground generation. In parallel, cross-attention maps derived from the foreground prompt T_{fg} highlight semantically relevant spatial regions. Combining these cues, we define the binary object mask m_{obj}^1 as:

$$m_{\text{obj}}(x, y) = \mathbf{1}[v_{\text{gb}}(x, y) < \tau_{\text{bg}} \wedge A_{\text{fg}}(x, y) > \tau_A], \quad (6)$$

¹The mask is primarily based on attention; minor processing variations depending on usage context are omitted here for clarity.

where τ_{bg} and τ_{attn} are predefined thresholds. This mask ensures accurate spatial localization of the foreground object. Here, $A_{\text{fg}} \in [0, 1]^{H/8 \times W/8}$ denotes the token-aggregated cross-attention map of the foreground prompt T_{fg} . For every latent location (x, y) , we set the object mask $m_{\text{obj}}(x, y)$ to 1 if (i) the green-background response $v_{\text{gb}}(x, y)$ falls below a background threshold τ_{bg} , and (ii) the attention weight $A_{\text{fg}}(x, y)$ exceeds an attention threshold τ_A . This conjunctive criterion retains only spatial positions that are simultaneously *not* dominated by the injected green background and *strongly attended* by the foreground textual tokens.

Cross-Attention Blending To achieve semantic coherence between the foreground and background, we modulate the cross-attention layers using the object mask m_{obj} . As shown in Fig. 3, the foreground prompt T_{fg} is applied only to the object region, and the background prompt T_{bg} to the rest. We obtain the mixed cross-attention tensor $A_{\text{mix}} \in \mathbb{R}^{H/8 \times W/8 \times d}$ by a pixel-wise convex combination of the foreground-conditioned attention A_{fg} and the background-conditioned attention A_{bg} :

$$A_{\text{mix}} = m_{\text{obj}} \odot A_{\text{fg}} + (1 - m_{\text{obj}}) \odot A_{\text{bg}}, \quad (7)$$

where $m_{\text{obj}} \in \{0, 1\}^{H/8 \times W/8}$ is the binary object mask based on the object’s spatial layout. The mask is broadcast over the d attention channels, ensuring that foreground tokens dominate inside the object region while background tokens govern elsewhere.

Denoising Process We initialize the composite generation with a blended latent that preserves object details while introducing new background content:

$$z'_{\text{all},T} = m_{\text{obj}} \odot (L_{\text{fg}} + \lambda \cdot n_{t_{\text{crop}}}) + (1 - m_{\text{obj}}) \odot z_T, \quad (8)$$

where L_{fg} is the foreground seedling latent, $n_{t_{\text{crop}}}$ is the predicted noise at the crop timestep, $z_T \sim \mathcal{N}(0, 1)$, and λ controls noise intensity. To further enhance spatial details, we apply a Laplacian filter to the seedling latent:

$$z_{\text{all},T} = m_{\text{obj}} \cdot (f(L_{\text{fg}}) + \lambda \cdot n_{t_{\text{crop}}}) + (1 - m_{\text{obj}}) \cdot z_T, \quad (9)$$

where $f(\cdot)$ is a high-pass filter. Denoising starts from $z_{\text{all},T}$, with noise blended at each timestep as follows:

$$n_t = \begin{cases} m_{\text{obj}} \odot n_{t_{\text{crop}}} + (1 - m_{\text{obj}}) \odot n_t & \text{if } t_{\text{crop}} \leq t, \\ n_t & \text{otherwise.} \end{cases} \quad (10)$$

This two-stage scheme fixes the foreground while allowing the background to evolve, ensuring semantic alignment and visual coherence. The composite image I_{all} is obtained at the final step, and the intermediate latent L_{bg} at timestep t_{crop} is passed to the following background generation phase.

3.3 Background Generation with Noise Transplantation and Cultivation

In this final phase, we generate the background image I_{bg} using the seedling latent L_{bg} from the composite generation and the background prompt T_{bg} . Similar to the previous phase, we transplant the latent into the initial noise and guide the denoising process with a spatial mask.

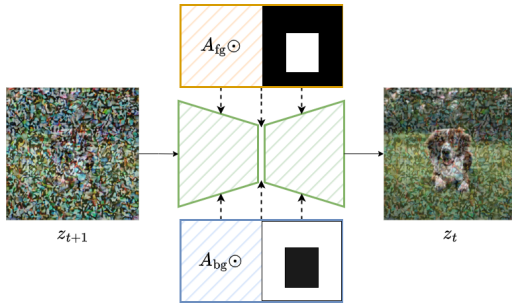


Figure 3: Illustration of the cross-attention blending mechanism. The foreground prompt is applied to object regions m_{obj} , while the background prompt is applied to non-object regions $1 - m_{\text{obj}}$. This enables precise control over foreground-background composition, ensuring cohesive integration of both layers in the final composite scene.

We define the background region as the complement of the object mask, $1 - m_{\text{obj}}$, ensuring that the foreground remains unaffected during the background generation. The initial latent is defined as:

$$z_{\text{bg},T} = (1 - m_{\text{obj}}) \odot (L_{\text{bg}} + \lambda \cdot n_{t_{\text{crop}}}) + m_{\text{obj}} \odot z_T, \quad (11)$$

where $z_T \sim \mathcal{N}(0, 1)$ and λ controls the influence of the foreground. Denoising starts from $z_{\text{bg},T}$ using a noise blending strategy. During early steps $t_{\text{crop}} \leq t$, we fix the background while allowing the foreground to evolve freely:

$$n'_t = \begin{cases} (1 - m_{\text{obj}}) \odot n_{t_{\text{crop}}} + m_{\text{obj}} \odot n_t & \text{if } t_{\text{crop}} \leq t, \\ n_t & \text{otherwise.} \end{cases} \quad (12)$$

This strategy enables independent background cultivation while maintaining spatial and semantic coherence with the fixed foreground. The resulting image I_{bg} exhibits consistent lighting, structure, and alignment with the composite.

4 Experiments

4.1 Experimental Setup

We adopt SDXL (Podell et al. 2023) as LDM for all experiments and generate images at a resolution of 1024×1024 using the EulerDiscrete scheduler (Karras et al. 2022) with 50 denoising steps. The guidance scale is set to 7.5 for foreground generation and 5.0 for all other cases. To extract the intermediate latent for seedling noise L_{fg} and L_{bg} , we set $r_{\text{crop}} = 0.5$, corresponding to the halfway point of the total denoising process. We compare TAUE with representative layer-wise generation baselines, including the fine-tuned method LayerDiffuse (Zhang and Agrawala 2024)², and the training-free method Alfie (Quattrini et al. 2024)³, combined with a background generation pipeline based on outpainting and inpainting (Zhang, Rao, and Agrawala 2023). Other existing methods were not included in our comparison, as their model weights or datasets are not publicly available, precluding reproducible evaluation.

²<https://github.com/Illyasviel/LayerDiffuse>

³<https://github.com/aimagelab/Alfie>

4.2 Dataset and Metrics

We construct a benchmark of 1770 images filtered from the MS-COCO dataset (Lin et al. 2014), considering limitations of existing methods in handling multi-object generation and extremely small objects. Specifically, we exclude samples where `iscrowd = true` or the bounding box area is less than 0.03 relative to image size. This ensures each image contains a single, reasonably sized foreground object suitable for fair comparison. To generate separate prompts for foreground T_{fg} and background T_{bg} , we employ Phi-3 (Abdin et al. 2024), a language model-based prompt captioning tool. To evaluate overall image quality, we use Fréchet Inception Distance (FID). For semantic consistency, we compute CLIP-Text (CLIP-T) and CLIP-Image (CLIP-I) similarity scores (Hessel et al. 2021), which assess alignment with the textual description and visual fidelity, respectively. To further evaluate the disentanglement of foreground and background from complete scenes, we compute PSNR, SSIM, and LPIPS (Zhang et al. 2018) scores between corresponding regions of the composite image and the individually generated foreground and background layers.

4.3 Qualitative Result

Fig. 4 presents qualitative results of our method and existing methods. Each method outputs foreground, background, and composite images for the same prompt. Alfie with inpainting, a training-free pipeline, generates the background via outpainting followed by inpainting after foreground generation. However, this often causes foreground features to bleed into the background due to mask misalignment and excessive outpainting. As a result, background images frequently contain residual foreground traces, thereby compromising layer independence. LayerDiffuse, a fine-tuned model, produces better separation and fewer artifacts. However, it still suffers from loss of foreground detail and imperfect semantic harmonization. Composite images occasionally exhibit lighting or shadow inconsistencies between layers.

In contrast, our TAUE generates all layers from a shared latent space via NTC, ensuring semantic and structural coherence without requiring fine-tuning. The resulting foreground, background, and composite outputs remain visually consistent, with no conflicts or missing elements. Notably, harmonization emerges naturally, as all layers are derived from successive noise injections, rather than mask-based composition or attention blending.

4.4 Quantitative Result

As shown in Tab. 2, TAUE achieves the best image quality among training-free methods across all metrics. Our method outperforms the fine-tuned LayerDiffuse in FID and CLIP-S, indicating superior visual fidelity and stronger alignment with textual prompts. While LayerDiffuse slightly leads in CLIP-I, TAUE remains highly competitive overall.

For layer-wise reconstruction, TAUE achieves the highest foreground accuracy across all metrics (PSNR, SSIM, LPIPS), demonstrating that the transplanted seedling noise effectively preserves object details. Background reconstruction scores are slightly lower than those of Alfie with

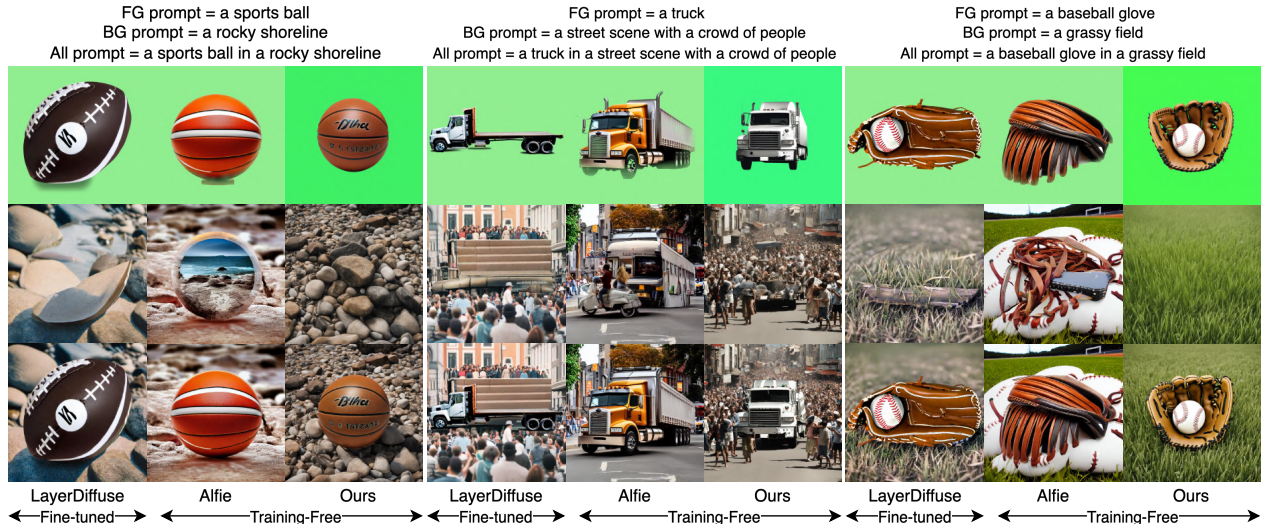


Figure 4: Qualitative comparison of layer-wise image generation. For each case, we show the foreground, background, and composite image generated by LayerDiffuse (Zhang and Agrawala 2024), Alfie (Quattrini et al. 2024), and our method. TAUE consistently produces spatially aligned and semantically coherent multi-layer outputs, achieving realistic integration of foreground and background without fine-tuning or inpainting.

	Overall Quality			Layer-wise Reconstruction Quality					
	FID ↓	CLIP-I ↑	CLIP-S ↑	PSNR _{fg} ↑	PSNR _{bg} ↑	SSIM _{fg} ↑	SSIM _{bg} ↑	LPIPS _{fg} ↓	LPIPS _{bg} ↓
<i>Fine-tuning Methods</i>									
LayerDiffuse	61.46	<u>0.653</u>	0.312	14.78	32.76	0.828	0.957	0.323	<u>0.039</u>
<i>Training-free Methods</i>									
Alfie + inpainting	85.93	0.644	0.302	15.32	<u>27.45</u>	0.778	<u>0.947</u>	0.254	0.019
Ours	<u>60.53</u>	0.646	<u>0.323</u>	<u>20.46</u>	25.86	<u>0.901</u>	0.895	<u>0.137</u>	0.106
<i>Application w/ Layout Specification</i>									
Ours	55.59	0.655	0.329	23.82	23.55	0.969	0.863	0.045	0.138

Table 2: Quantitative comparison of overall image quality and layer-wise reconstruction performance. We report FID, CLIP-I, and CLIP-S for holistic quality, and PSNR, SSIM, and LPIPS for foreground (fg) and background (bg) reconstruction. Lower is better for FID and LPIPS (↓), and higher is better for CLIP, PSNR, and SSIM (↑). The best and second-best results are shown in bold and underlined, respectively. TAUE outperforms both fine-tuned and training-free baselines across most metrics, with its layout-aware variant achieving the best foreground fidelity and overall quality.

inpainting and LayerDiffuse, both of which benefit from reusing unmasked background pixels—an advantage that artificially boosts their scores. In contrast, TAUE performs denoising entirely from scratch, relying solely on intermediate seedling noise without reusing any pixel values. This increases the difficulty of the task, making it more challenging, and reduces the likelihood of regenerating the foreground object in exactly the same position and structure. Nevertheless, TAUE maintains a strong background quality and overall consistency, confirming that our NTC reliably guides generation without requiring fine-tuning or additional data.

5 Applications

We demonstrate the utility of TAUE in three applications: layout and size control, multi-object generation with disentangled attributes, and background replacement. These capa-

bilities are essential in creative workflows that demand spatial precision, semantic separation, and iterative editing. As shown in Fig. 5 and Table 2, TAUE produces high-quality, controllable outputs without requiring fine-tuning or additional training data.

Layout and Size Control Existing layer-wise image generation models often produce centrally aligned, uniformly sized objects due to limited spatial conditioning (Zhang and Agrawala 2024; Quattrini et al. 2024). Controlling object scale via prompts or layout models often lacks consistency and flexibility. TAUE addresses these limitations by injecting user-defined bounding boxes, which specify the foreground object’s location and size. This guides seedling noise transplantation and denoising to generate semantically coherent content within the desired region.

As shown in Tab. 2, the layout-aware TAUE im-

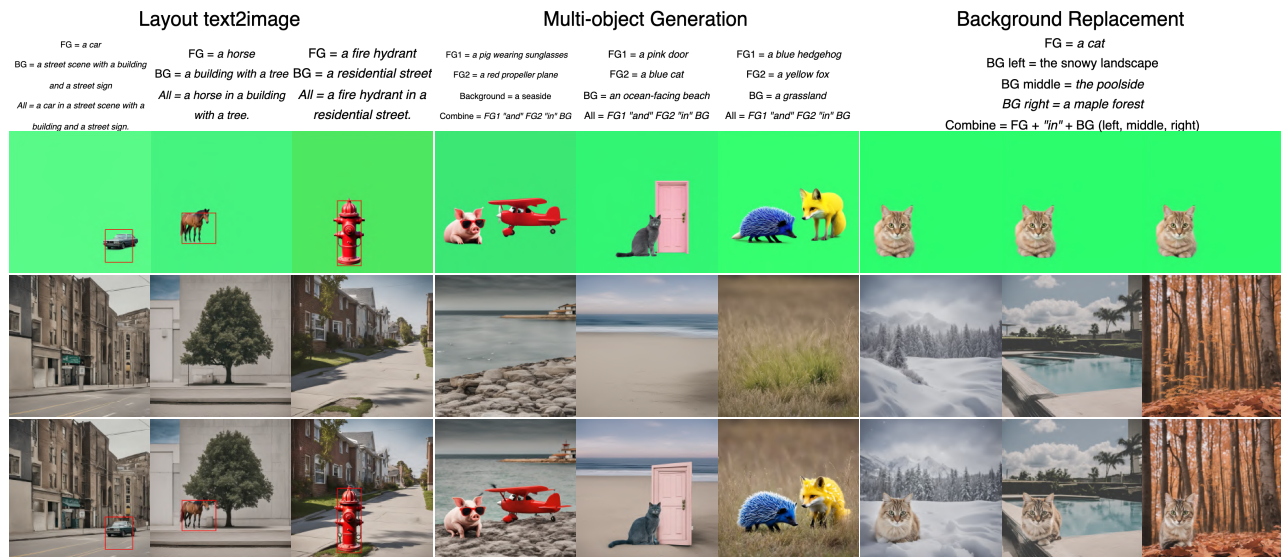


Figure 5: Applications of TAUE. TAUE enables (a) *Layout and Size Control* by injecting bounding box constraints to specify the position and scale of the foreground object; (b) *Disentangled Multi-Object Generation* by transplanting seedling noise to multiple spatial locations, allowing compositionally coherent and semantically independent objects; and (c) *Background Replacement* by regenerating backgrounds while preserving the original foreground structure.

proves FID, CLIP-I, CLIP-S, and foreground reconstruction (PSNR, SSIM, LPIPS). Explicit size control also enhances alignment with object semantics, yielding more accurate object scales. While background reconstruction is slightly lower due to full denoising instead of pixel reuse, this trade-off improves harmonization and realism. These results show that TAUE enables user-driven spatial generation without training, making it practical for layout-aware applications.

Disentangled Multi-Object Generation Text-to-image models often suffer from attribute entanglement when generating multiple objects in a single prompt like incorrect color or shape assignments. Prior works (Zhang and Agrawala 2024) mitigate this by sequential generation and compositing, but incur high inference cost and blending artifacts.

TAUE introduces an efficient alternative by transplanting seedling noise to multiple spatial locations in the latent space. Each transplanted latent preserves its object semantics, enabling simultaneous generation of multiple, disentangled objects in a single denoising process. As shown in Fig. 5, our method produces multi-object scenes with semantic separation and spatial consistency, without requiring layout models or additional training. This facilitates controllable scene composition at scale, with minimal overhead.

Background Replacement Conventional diffusion models regenerate the full image to modify the background, which risks altering the foreground due to entangled representations. TAUE resolves this by decoupling foreground and background generation via latent transplantation. Once the foreground object is generated, its seedling noise can be retained and reused to synthesize a new background independently. This ensures a consistent foreground appearance and layout. Additionally, adjusting the transplantation coordinates allows repositioning of the object across backgrounds,

enabling interactive layout-aware editing.

Unlike previous methods that rely on handcrafted prompts or model retraining, TAUE enables seamless background editing in a training-free, zero-shot manner. This enables rapid iteration and fine-grained control in creative workflows, such as UI design and ad generation.

6 Conclusion

We presented TAUE, a novel training-free framework for layer-wise image generation that enables the synthesis of disentangled foreground and background. By introducing the concept of NTC, TAUE modifies the initial noise within the diffusion process to maintain semantic coherence across layers without requiring any fine-tuning or external datasets. Extensive experiments demonstrate that TAUE achieves performance comparable to fine-tuned models while offering greater flexibility and efficiency. Furthermore, we presented practical applications, such as layout and size control, multi-object generation, and background replacement, highlighting TAUE’s potential for real-world creative workflows. We believe that TAUE opens up new avenues for controllable, modular, and accessible image generation in both research and professional domains.

Limitation In cases requiring high-fidelity foreground preservation, e.g., when the exact shape, color, or pixel-level structure of the foreground must remain unchanged—TAUE may underperform compared to inpainting-based approaches that modify the background while preserving the foreground. Future work should explore ways to better control this behavior, such as selectively freezing foreground features during compositing or introducing constraints to balance semantic adaptation and structural preservation. Addressing this trade-off between harmonization and fi-

delity will be crucial to expanding TAUE’s applicability in precision-critical tasks.

References

- Abdin, M.; Aneja, J.; Awadalla, H.; Awadallah, A.; Awan, A. A.; Bach, N.; Bahree, A.; Bakhtiari, A.; Bao, J.; Behl, H.; et al. 2024. Phi-3 technical report: A highly capable language model locally on your phone. *arXiv preprint arXiv:2404.14219*.
- Ban, Y.; Wang, R.; Zhou, T.; Gong, B.; Hsieh, C.-J.; and Cheng, M. 2024. The Crystal Ball Hypothesis in diffusion models: Anticipating object positions from initial noise. *arXiv preprint arXiv:2406.01970*.
- Burgert, R. D.; Price, B. L.; Kuen, J.; Li, Y.; and Ryoo, M. S. 2024. Magick: A large-scale captioned dataset from matting generated images using chroma keying. In *Proceedings of the IEEE/CVF Conference on Computer Vision and Pattern Recognition*, 22595–22604.
- Chen, C.; Yang, L.; Yang, X.; Chen, L.; He, G.; Wang, C.; and Li, Y. 2024a. Find: Fine-tuning initial noise distribution with policy optimization for diffusion models. In *Proceedings of the 32nd ACM International Conference on Multimedia*, 6735–6744.
- Chen, S. X.; Vaxman, Y.; Ben Baruch, E.; Asulin, D.; Moreshet, A.; Lien, K.-C.; Sra, M.; and Sen, P. 2024b. Tino-edit: Timestep and noise optimization for robust diffusion-based image editing. In *Proceedings of the IEEE/CVF Conference on Computer Vision and Pattern Recognition*, 6337–6346.
- Dalva, Y.; Li, Y.; Liu, Q.; Zhao, N.; Zhang, J.; Lin, Z.; and Yanardag, P. 2024. LayerFusion: Harmonized Multi-Layer Text-to-Image Generation with Generative Priors. *arXiv preprint arXiv:2412.04460*.
- Eyring, L.; Karthik, S.; Roth, K.; Dosovitskiy, A.; and Akata, Z. 2024. ReNO: Enhancing One-step Text-to-Image Models through Reward-based Noise Optimization. *arXiv preprint arXiv:2406.04312*.
- Fontanella, A.; Tudosi, P.-D.; Yang, Y.; Zhang, S.; and Parisot, S. 2024. Generating compositional scenes via Text-to-image RGBA Instance Generation. *Advances in Neural Information Processing Systems*, 37: 43864–43893.
- Guo, X.; Liu, J.; Cui, M.; Li, J.; Yang, H.; and Huang, D. 2024. Initno: Boosting text-to-image diffusion models via initial noise optimization. In *CVPR*, 9380–9389.
- Han, W.; Lee, Y.; Kim, C.; Park, K.; and Hwang, S. J. 2025. Spatial Transport Optimization by Repositioning Attention Map for Training-Free Text-to-Image Synthesis. In *Proceedings of the Computer Vision and Pattern Recognition Conference*, 18401–18410.
- Hessel, J.; Holtzman, A.; Forbes, M.; Bras, R. L.; and Choi, Y. 2021. Clipscore: A reference-free evaluation metric for image captioning. *arXiv preprint arXiv:2104.08718*.
- Ho, J.; Jain, A.; and Abbeel, P. 2020. Denoising diffusion probabilistic models. *Advances in neural information processing systems*, 33: 6840–6851.
- Hu, X.; Peng, X.; Luo, D.; Ji, X.; Peng, J.; Jiang, Z.; Zhang, J.; Jin, T.; Wang, C.; and Ji, R. 2024. Diffumattng: Synthesizing arbitrary objects with matting-level annotation. In *European Conference on Computer Vision*, 396–413. Springer.
- Huang, D.; Li, W.; Zhao, Y.; Pan, X.; Zeng, Y.; and Dai, B. 2025a. PSDiffusion: Harmonized Multi-Layer Image Generation via Layout and Appearance Alignment. *arXiv preprint arXiv:2505.11468*.
- Huang, J.; Yan, P.; Cai, J.; Liu, J.; Wang, Z.; Wang, Y.; Wu, X.; and Li, G. 2025b. DreamLayer: Simultaneous Multi-Layer Generation via Diffusion Mode. *arXiv preprint arXiv:2503.12838*.
- Huang, R.; Cai, K.; Han, J.; Liang, X.; Pei, R.; Lu, G.; Xu, S.; Zhang, W.; and Xu, H. 2024. LayerDiff: Exploring Text-guided Multi-layered Composable Image Synthesis via Layer-Collaborative Diffusion Model. In *European Conference on Computer Vision*, 144–160. Springer.
- Izadi, A. M.; Hosseini, S. M. H.; Tabar, S. V.; Abdollahi, A.; Saghafian, A.; and Baghshah, M. S. 2025. Fine-Grained Alignment and Noise Refinement for Compositional Text-to-Image Generation. *arXiv preprint arXiv:2503.06506*.
- Kang, K.; Sim, G.; Kim, G.; Kim, D.; Nam, S.; and Cho, S. 2025. LayeringDiff: Layered Image Synthesis via Generation, then Disassembly with Generative Knowledge. *arXiv preprint arXiv:2501.01197*.
- Karras, T.; Aittala, M.; Aila, T.; and Laine, S. 2022. Elucidating the design space of diffusion-based generative models. *Advances in neural information processing systems*, 35: 26565–26577.
- Lin, T.-Y.; Maire, M.; Belongie, S.; Hays, J.; Perona, P.; Ramanan, D.; Dollár, P.; and Zitnick, C. L. 2014. Microsoft coco: Common objects in context. In *European conference on computer vision*, 740–755. Springer.
- Liu, Z.; Liu, Q.; Chang, C.; Zhang, J.; Pakhomov, D.; Zheng, H.; Lin, Z.; Cohen-Or, D.; and Fu, C.-W. 2024. Object-level scene deocclusion. In *ACM SIGGRAPH 2024 Conference Papers*, 1–11.
- Mao, J.; Wang, X.; and Aizawa, K. 2023a. Guided Image Synthesis via Initial Image Editing in Diffusion Model. *arXiv preprint arXiv:2305.03382*.
- Mao, J.; Wang, X.; and Aizawa, K. 2023b. Semantic-Driven Initial Image Construction for Guided Image Synthesis in Diffusion Model. *arXiv preprint arXiv:2312.08872*.
- Morita, R.; Frolov, S.; Moser, B. B.; Shirakawa, T.; Watanabe, K.; Dengel, A.; and Zhou, J. 2025. TKG-DM: Training-free Chroma Key Content Generation Diffusion Model. In *Proceedings of the Computer Vision and Pattern Recognition Conference*, 13031–13040.
- Podell, D.; English, Z.; Lacey, K.; Blattmann, A.; Dockhorn, T.; Müller, J.; Penna, J.; and Rombach, R. 2023. Sdxl: Improving latent diffusion models for high-resolution image synthesis. *arXiv preprint arXiv:2307.01952*.
- Pu, Y.; Zhao, Y.; Tang, Z.; Yin, R.; Ye, H.; Yuan, Y.; Chen, D.; Bao, J.; Zhang, S.; Wang, Y.; et al. 2025. Art: Anonymous region transformer for variable multi-layer transparent image generation. In *Proceedings of the Computer Vision and Pattern Recognition Conference*, 7952–7962.

- Qi, Z.; Bai, L.; Xiong, H.; and Xie, Z. 2024. Not all noises are created equally: Diffusion noise selection and optimization. *arXiv preprint arXiv:2407.14041*.
- Quattrini, F.; Pippi, V.; Cascianelli, S.; and Cucchiara, R. 2024. Alfie: Democratising RGBA Image Generation with No. In *European Conference on Computer Vision*, 38–55. Springer.
- Rombach, R.; Blattmann, A.; Lorenz, D.; Esser, P.; and Ommer, B. 2022. High-resolution image synthesis with latent diffusion models. In *Proceedings of the IEEE/CVF conference on computer vision and pattern recognition*, 10684–10695.
- Shirakawa, T.; and Uchida, S. 2024. NoiseCollage: A Layout-Aware Text-to-Image Diffusion Model Based on Noise Cropping and Merging. In *CVPR*, 8921–8930.
- Song, J.; Meng, C.; and Ermon, S. 2020. Denoising diffusion implicit models. *arXiv preprint arXiv:2010.02502*.
- Tudosiu, P.-D.; Yang, Y.; Zhang, S.; Chen, F.; McDonagh, S.; Lampouras, G.; Iacobacci, I.; and Parisot, S. 2024. Mulan: A multi layer annotated dataset for controllable text-to-image generation. In *Proceedings of the IEEE/CVF Conference on Computer Vision and Pattern Recognition*, 22413–22422.
- Wang, R.; Huang, H.; Zhu, Y.; Russakovsky, O.; and Wu, Y. 2024. The Silent Assistant: NoiseQuery as Implicit Guidance for Goal-Driven Image Generation. *arXiv preprint arXiv:2412.05101*.
- Winter, D.; Cohen, M.; Fruchter, S.; Pritch, Y.; Rav-Acha, A.; and Hoshen, Y. 2024. Objectdrop: Bootstrapping counterfactuals for photorealistic object removal and insertion. In *European Conference on Computer Vision*, 112–129. Springer.
- Wu, T.; Si, C.; Jiang, Y.; Huang, Z.; and Liu, Z. 2024. Freeinit: Bridging initialization gap in video diffusion models. In *European Conference on Computer Vision*, 378–394. Springer.
- Xu, K.; Zhang, L.; and Shi, J. 2024. Good Seed Makes a Good Crop: Discovering Secret Seeds in Text-to-Image Diffusion Models. *arXiv preprint arXiv:2405.14828*.
- Yang, J.; Liu, Q.; Li, Y.; Kim, S. Y.; Pakhomov, D.; Ren, M.; Zhang, J.; Lin, Z.; Xie, C.; and Zhou, Y. 2025. Generative Image Layer Decomposition with Visual Effects. In *Proceedings of the Computer Vision and Pattern Recognition Conference*, 7643–7653.
- Zhang, L.; and Agrawala, M. 2024. Transparent image layer diffusion using latent transparency. *arXiv preprint arXiv:2402.17113*.
- Zhang, L.; Rao, A.; and Agrawala, M. 2023. Adding conditional control to text-to-image diffusion models. In *Proceedings of the IEEE/CVF international conference on computer vision*, 3836–3847.
- Zhang, L.; Wen, T.; and Shi, J. 2020. Deep image blending. In *Proceedings of the IEEE/CVF winter conference on applications of computer vision*, 231–240.
- Zhang, R.; Isola, P.; Efros, A. A.; Shechtman, E.; and Wang, O. 2018. The Unreasonable Effectiveness of Deep Features as a Perceptual Metric. In *CVPR*.
- Zhang, X.; Zhao, W.; Lu, X.; and Chien, J. 2023. Text2layer: Layered image generation using latent diffusion model. *arXiv preprint arXiv:2307.09781*.
- Zhou, Z.; Shao, S.; Bai, L.; Xu, Z.; Han, B.; and Xie, Z. 2024. Golden noise for diffusion models: A learning framework. *arXiv preprint arXiv:2411.09502*.
- Zou, K.; Feng, X.; Wang, P.; Huang, T.; Huang, Z.; Haihang, Z.; Zou, Y.; and Li, D. 2025. Zero-Shot Subject-Centric Generation for Creative Application Using Entropy Fusion. *arXiv preprint arXiv:2503.10697*.

A Ablation Study

We analyze the contribution of each component through controlled ablations.

A.1 High-Pass Filtering for Composite Initialization

To preserve object structure transferred by the seedling latent, we apply a Laplacian high-pass filter to L_{fg} before the composite denoising begins (Sec. 3.2). Quantitatively, removing the filter (*50% w/o High-pass*) slightly increases some pixel-based reconstruction scores (e.g., PSNR_{fg} 23.92, SSIM_{fg} 0.970) but hurts holistic quality (FID 55.79 vs. 55.59 and lower CLIP-S), and leads to visible artifacts such as softened boundaries and occasional duplicate instances (Fig. 6, Tab. 3). With the filter, high-frequency cues in the transplanted latent survive the earliest steps, allowing the composite generator to *use* the foreground semantics to build a coherent scene around it—e.g., laying out a road consistent with a bus foreground rather than “cut-and-paste” blending. Empirically, this yields sharper contours and more faithful materials while keeping strong perceptual-based reconstruction (LPIPS_{fg} 0.045, LPIPS_{bg} 0.138) and the best overall FID/CLIP.

A.2 Choice of Crop Ratio

We evaluate three crop ratios for extracting the seedling latent—25%, 50%, and 75% of the scheduler trajectory (Fig. 7, Tab. 3). At **25% (early)**, the latent is still close to Gaussian, yielding prompt-irrelevant residuals and the lowest alignment (CLIP-I 0.640, CLIP-S 0.321) and weak reconstruction (PSNR_{bg} 19.70, LPIPS_{bg} 0.284). At **75% (late)**, the foreground is already near-complete when transplanted; this inflates reconstruction metrics (PSNR_{fg} 24.33, SSIM_{fg} 0.974; PSNR_{bg} 25.02, LPIPS_{bg} 0.091) but degrades harmonization and yields a more “independently generated” foreground that fails to adapt to the background (slightly worse FID 56.48 and comparable CLIP). The **50% (mid)** setting strikes the best trade-off: the object is formed enough to steer composition yet malleable enough to integrate with the background, giving the best holistic quality (FID 55.59, CLIP-I 0.655, CLIP-S 0.329) while maintaining strong reconstruction.

B Additional Results

Figure 8 provides additional qualitative examples across diverse categories. For each case we show the *Foreground Object*, the *Background*, and the final *Composite*. TAUE maintains semantic and spatial consistency among all three outputs while preserving fine object details and realistic scene context.

Method	Overall Quality			Layer-wise Reconstruction Quality					
	FID ↓	CLIP-I ↑	CLIP-S ↑	PSNR _{fg} ↑	PSNR _{bg} ↑	SSIM _{fg} ↑	SSIM _{bg} ↑	LPIPS _{fg} ↓	LPIPS _{bg} ↓
Ours (50% + High-pass)	55.59	0.655	0.329	23.82	23.55	0.969	0.863	0.045	0.138
50% w/o High-pass	55.79	0.654	0.328	23.92	23.59	0.970	0.862	0.045	0.139
75% (late)	56.48	0.653	0.328	24.33	25.02	0.974	0.904	0.041	0.091
25% (early)	55.70	0.640	0.321	21.12	19.70	0.953	0.750	0.059	0.284

Table 3: **Ablation on high-pass filtering and crop ratio.** Our default (50% + *High-pass*) achieves the best holistic quality (lower FID, higher CLIP) while keeping strong reconstruction. Removing the high-pass slightly improves some reconstruction metrics but visibly hurts perceptual quality (edge softness / occasional duplications). Extracting the seedling too late (75%) boosts reconstruction scores but degrades harmonization; too early (25%) leaves residual noise and lowers text alignment.

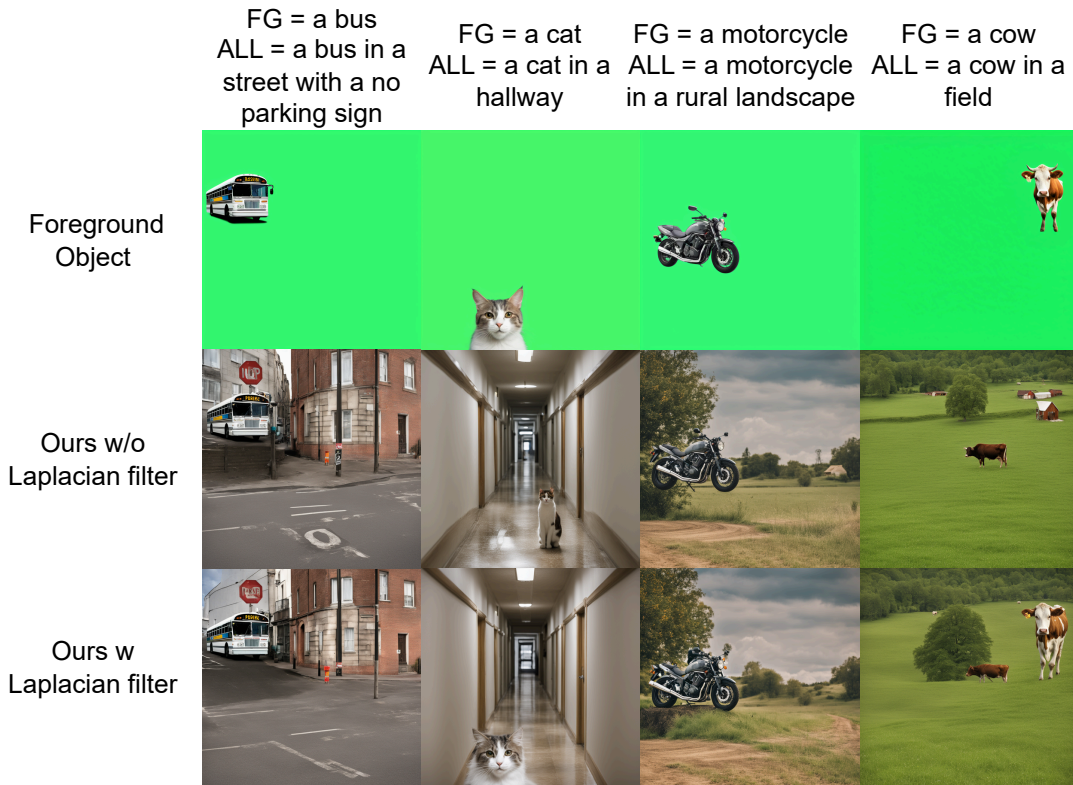


Figure 6: **Ablation of the Laplacian high-pass filter.** Each column shows one prompt. Row 1: composite results *without* the filter sometimes contain spurious duplicates or softened boundaries. Row 2: applying the filter preserves high-frequency cues in the transplanted latent, producing one clean instance with sharper edges and textures. Best viewed zoomed in.

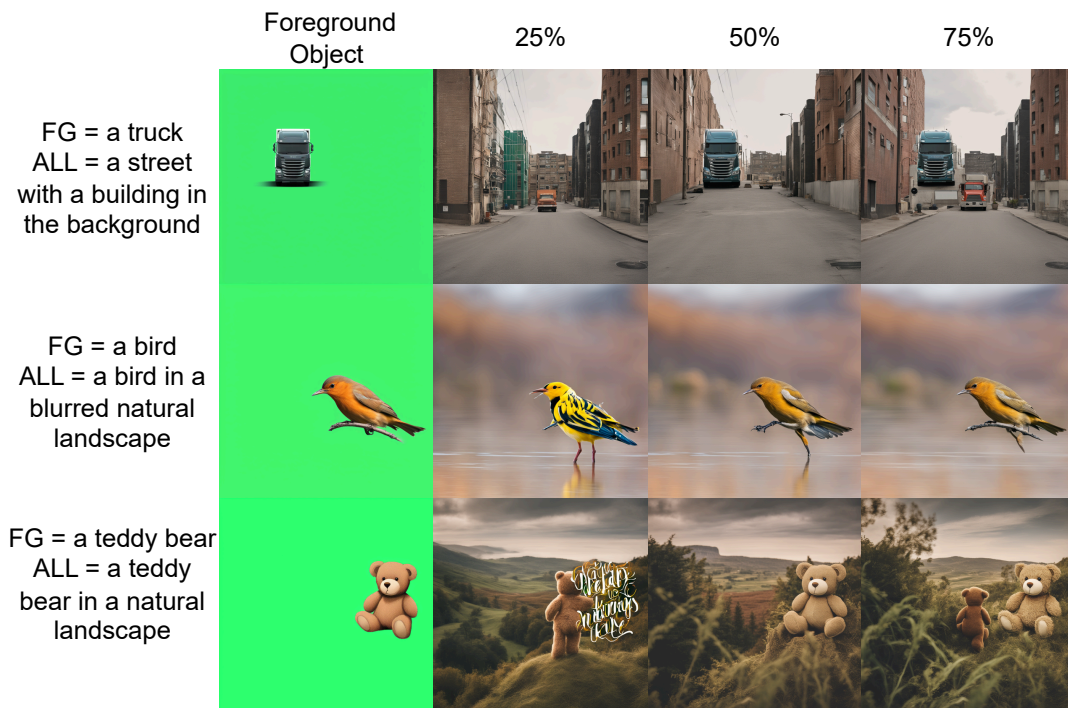


Figure 7: **Effect of crop ratio (25%, 50%, 75%)**. Columns correspond to the ratio at which the seedling latent is extracted from the denoising trajectory. At 25% (early), prompt-irrelevant residual noise appears; at 75% (late), the foreground fails to harmonize with the regenerated background. The mid-point 50% consistently gives the most coherent composite with accurate lighting and depth.

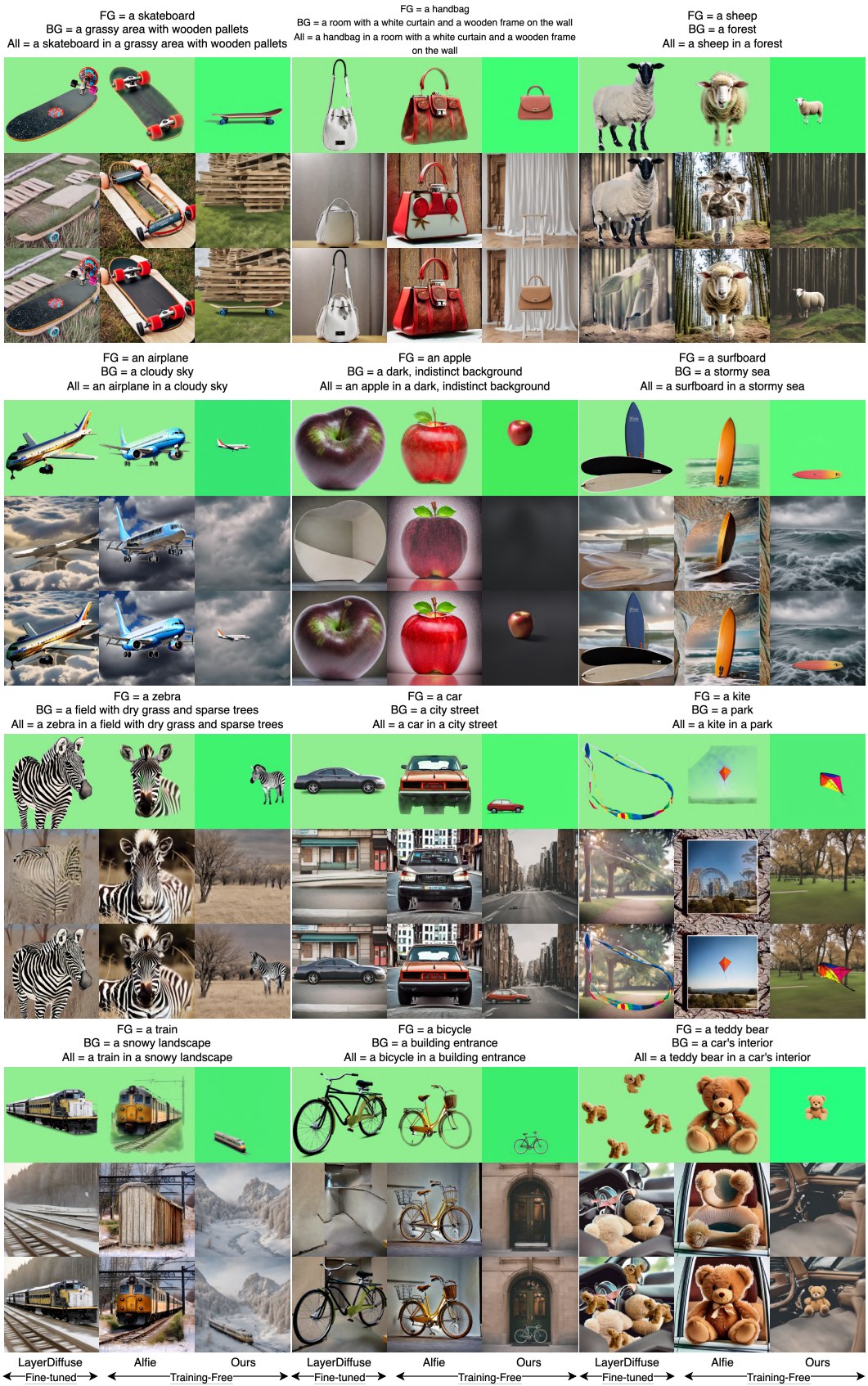


Figure 8: **More qualitative results.** Each triplet shows foreground, background, and composite. Across vehicles, animals, man-made objects, and natural scenes, TAUE produces crisp foregrounds, harmonized backgrounds, and composites with consistent geometry, lighting, and shadows—without fine-tuning or inpainting.